# Docking and Molecular Dynamics Simulations Reveal A Possible Site of Interaction of Olive Leaf Extract Hydroxytyrosol with Polyunsaturated Fatty Acid 5-Lipoxygenase Human Enzyme

Maria Valentini, Enrico Pieroni, Alessandro Concas, and Massimo Pisu

## **ABSTRACT**

The polyphenol hydroxytyrosol (HT), a molecule easily extracted from olive oil production waste, has well known antioxidant and anti-inflammatory properties. In literature various bioassays points to a clear inhibitory effects on the polyunsaturated fatty acid 5-lipoxygenase enzyme (LOX5) which is a current target for pharmaceutical intervention for various inflammatory diseases. We have investigated the hypothesis of direct interaction of HT with LOX5 through blind docking and a 200 nanoseconds long molecular dynamics. Analysis of the results highlights the stability of the interaction of HT in the putative binding site with LOX5. This is in accord with the hypothesis of an allosteric way of action of HT to inhibit the activity of the LOX5 also suggesting the use of HT structure as a scaffold to design LOX5 inhibitors with improved activity and specificity.

**Keywords:** Docking, molecular dynamics, hydroxytyrosol, olive leaf extract, LOX5\_HUMAN, 5-lipoxygenase.

Published Online: March 23, 2022

ISSN: 2684-5199

DOI: 10.24018/ejbio.2022.3.2.345

#### M. Valentini\*

Center for Advanced Studies, Research and Development in Sardinia (CRS4), Pula, Cagliari, Italy.

(e-mail: maria@crs4.it)

#### E. Pieroni

Center for Advanced Studies, Research and Development in Sardinia (CRS4), Pula, Cagliari, Italy.

#### A. Concas

Department of Mechanical, Chemical and Materials Engineering, University of Cagliari, Italy.

#### M. Pisu

Center for Advanced Studies, Research and Development in Sardinia (CRS4), Pula, Cagliari, Italy.

\*Corresponding Author

# I. Introduction

Large amounts of agro-industrial wastes, characterized by relatively high concentration of potentially useful bioactive molecules, are currently produced worldwide (Sadh et al., 2018). Therefore, the extraction of such biomolecules and their subsequent valorization in different market sectors, represent today crucial goals in view of the implementation of the "circular economy" paradigm in the modern society (Romani et al., 2016). In fact, this approach would reduce the environmental concerns deriving from waste storage, while an immediate economic benefit would be achieved by "closing the loop" of agricultural product lifecycle. Moreover, exploitation in the biomedical and pharmaceutical fields will provide further benefit, namely the improvement of human health.

Particularly the latter one is the case of polyphenolic molecules, which can be found in several kinds of agroindustrial wastes with concentrations up to 100 ppm and are characterized by many therapeutic properties (Romani et al., 2016). In fact, they are typically characterized by high antioxidative power, and are thus able to decrease general inflammation levels (Corrêa and Rogero 2019), reduce cardiovascular diseases and aging effects (Tomé-Carneiro and Visioli, 2016), relieve arthritis symptoms (Christman and Gu, 2020) and contribute to the treatment of several pathologies associated to free radicals oxidation including cancer (Romani et al., 2016; Zhou et al., 2016).

Among polyphenols, hydroxytyrosol dihydroxyphenil-ethanol, HT) is one of those with the highest antioxidant activity that can be found in olive oil. Moreover, high amounts of HT can be extracted from byproducts of the olive oil production process such as olive mill wastewaters (Bertin et al., 2011) or olive leaves (Zurob et al., 2020). According to the literature, olive oil is mostly (~ 98% of world production) produced in the countries of the Mediterranean basin and leads to the generation of oil mill wastewater (Frascari et al., 2016). Since olive mill wastewaters may cause important environmental concerns (Bertin et al., 2011) and HT, at purity greater than 98%, can be sold in the market with prices ranging from 7870 US\$ to 10360 US\$ (SIGMA ALDRICH 2020), it is apparent that the extraction and reuse of HT from waste might lead to a winwin situation in both environmental and economic terms.

The high selling price of HT is due to the difficulty of its extraction and purification but even to its high potentialities in the biomedical and pharmaceutical sector (Frascari et al., 2016). Namely, HT proved to have an antioxidant activity two times more than coenzyme Q10 and ten times more than epicatechin, thus being, along with gallic acid, one of the

natural molecules with the highest antioxidant power (Zurob et al., 2020). In addition, HT has shown several antiinflammatory and antioxidant activities in vitro that may be responsible for the preventive properties of chronic degenerative diseases associated to olive oil (Han et al., 2009). Since chronic inflammation and oxidative stress are implicated in the onset of many chronic degenerative pathologies such as diabetes, cancer, cardiovascular, autoimmune and neurodegenerative diseases, it is clear that the use of such a powerful antioxidant can be helpful to prevent or to treat the above-mentioned diseases (Han et al., 2009).

Actually, relevant potentialities of HT as a synergic supplement during the treatment of different types of cancer are reported in the literature. In fact, in vitro studies demonstrated that HT could induce apoptosis in breast (Han et al., 2009), prostate (Zubair et al., 2017), pancreatic (Goldsmith et al., 2018) and colorectal (Sun et al., 2014) cancer cells. Relevant studies have also shown that HT can be helpful to prevent cardiovascular and metabolic diseases (Bulotta et al., 2014). Moreover, it has been reported that HT supplementation has antidiabetic effects in rats (Jemai et al., 2009). Finally, recent studies have demonstrated that HT can interfere with the growth of amyloid fibril growth by promoting their disaggregation and thus resulting potentially effective in the treatment of Alzheimer's disease (Leri et al., 2019).

Beneficial effects of HT on several other diseases can be found in the literature and, in all cases, they seem to be somehow related to HT high antioxidant and antiinflammatory properties (Hu et al., 2014). The enzyme 5lipoxygenase (UniProtKB: P09917 LOX5 HUMAN) (LOX5) is in charge of the first steps in the biosynthesis of pro-inflammatory leukotrienes and is then considered a very promising pharmacological target for the treatment of inflammatory diseases (e.g. asthma and allergic rhinitis) (Pergola and Werz, 2010). Different assays on oleoderivates signaled the inhibitory effect of HT on LOX5, and HT was identified as the most potent derivative with an IC50 of 13–15  $\mu M$  (Kohyama et al., 1997; De La Puerta et al., 1999). Another assay (Vougogiannopoulou et al., 2014) found about 48% inhibition at 10 µM for HT. Those values of IC50 are one order of magnitude greater than the only clinical approved LOX5 inhibitor, zileuton with an IC50 of  $(1 \pm 0.5)$ μM, reflecting the promising potential of HT as an antiinflammatory agent. Metabolism studies (Marković et al., 2019) show that HT and its metabolites have a widespread and effective distribution in tissues such as muscle, testis, liver, and brain besides being accumulated in the kidney and liver (D'Angelo et al., 2001; Serra et al., 2012).

Despite the variety of interesting effects of HT on human health discussed above, to the best of our knowledge, in the current literature there is still a lack of specific studies at molecular level on possible mechanisms of interaction of such an antioxidant with living cells and in particular through the enzyme LOX5. These considerations led us to the decision to undertake a computational study to investigate the eventual direct binding of HT to LOX5.

## II. MATERIALS AND METHODS

## A. Molecular Models of LOX5 and HT

The 5-LOX mutant human enzyme crystal structure is present in the PDB database with code 308Y at 2.4 A resolution (Gilbert et al., 2011). This structure is a dimer of two homologous chains A and B and presents the mutation of three amino acids, namely LYS653 LYS654 LYS655 mutated to GLU653 ASN654 LEU655, to stabilize the structure.

In this study we have prepared two monomeric structure models: i) the stable enzyme structure with the Fe<sup>++</sup> in the catalytic site, as resulting from the PDB file 3O8Y and ii) LOX5 noFe, namely the previous crystal structure in the apo form, where the Fe<sup>++</sup> is removed from the catalytic site.

The structure of HT (HT CAS-10597-60-1) has been obtained from the HT mol2 file in ZINC database, with code ZINC2379217 (Sterling and Irwin, 2015). The threedimensional model of HT has been optimized through an energetic minimization performed by using the PRODRG server (Schüttelkopf and Van Aalten, 2004).

# B. Docking

The initial structure was minimized through PRODRG server, then blind ensemble docking calculations were performed using AutoDock VINA (Trott and Olson 2009). As we were interested in finding binding poses of the ligand HT on the whole region of LOX5, docking was performed within a rectangular search space of size 90Å×90Å×113Å enclosing the whole protein. The exhaustiveness parameter was set to 800 (100 times the default) in order to improve the sampling within the large box used (27 times the suggested volume), while the flexibility of the ligands was considered by activating torsional angles in AutoDock VINA in the starting structure. In ligand preparation, Gasteiger charges were computed, nonpolar hydrogen atoms were merged, torsion angles for all rotatable bonds were set as flexible. Similarly, protein files were prepared using automated functions of the AutoDock tools that added all hydrogen atoms, computed Gasteiger charges, and merged non-polar hydrogen atoms.

The same docking protocol with the same parameters has been performed to obtain the best poses respectively for: i) the enzyme model as found in PDB 3O8Y structure and ii) the apo form of the enzyme (i.e. without the non-heme iron ion (Fe<sup>++</sup>) in the catalytic site).

# C. Molecular Dynamics

We performed molecular dynamic simulations of the complex LOX5-HT using NAMD (Phillips et al., 2005) starting from the best pose for the LOX5 apo form structure, obtained in the previous docking study. VMD software was used to generate PSF file for the complex (Humphrey et al., 1996).

The CGENFF topology and parameters for HT were generated via the PARAMCHEM (Vanommeslaeghe et al., 2010). The system has been solvated in a cubic water box, using the 3-points water molecules model (TIP3P), with 9250 explicit water molecules. The box size was chosen so that there was a distance of 10 Å between the protein surface and the edges of the periodic box. Finally the system was neutralized by adding 22 SOD atoms.

The particle mesh Ewald (PME) method was used to calculate long-range electrostatic interactions. The SHAKE method was used to constrain all bonds involving hydrogen atoms. The system first performed 10000 steps of steepest descent with energy minimization and it has been equilibrated in the NPT ensemble with the Nosé-Hoover method (Nosé, 1984) to maintain a constant temperature of 310 K.

The production dynamics has been performed in the NVT ensemble with a timestep of 2fs for a total time life of 217 ns. Frames and energies were saved every 10 ps for a total of 21777 frames.

Molecular Dynamics (MD) trajectory has been analyzed through the Python package for the rapid analysis of molecular dynamics simulations MDAnalysis (Michaud-Agrawal et al., 2011) in particular using the Hydrogen Bond and Distance analysis modules.

## III. RESULTS AND DISCUSSION

LOX5 structure is characterized by three main domains usually identified as the N-terminal domain from residue 1 to 110, the interdomain linker from residue 111 to 119 and the much larger C-terminal domain from residue 120 to 669. The N-terminal regulatory domain consists mainly of beta-sheets (Gilbert et al., 2020) and is responsible for bringing the enzyme in proximity of its substrate within the nuclear membrane.

The C-terminal domain is mainly formed by alpha-helix and harbors the catalytic site with a non-heme catalytic iron coordinated by the three Histidines (367, 372 and 550) and the main-chain carboxylate of ILE673. In the crystal structure the active site is an elongated cavity without clear access to bulk solvent In particular, it is a partial U shaped cavity lined with highly conserved Leu and Ile residues, namely LEU368, LEU373, LEU414, LEU607 and ILE406, and appears to follow the current structural consensus for LOX enzymes (Newcomer and Brash 2015), except for the arched helix that shields access to the catalytic iron, with vertex LEU414, PHE421 and LEU420, which is shorter than other enzymes in the LOX family.

## A. Docking Results

We have performed two different docking experiments: one with the enzyme LOX5 in its stable form and the other considering stable LOX5 apo form, i.e. without the iron ion Fe<sup>++</sup> in the active site (LOX5\_noFe).

The two best poses from the two different docking studies have a reciprocal RMSD of 0.377 Å, which means that they practically overlap. The ligand configuration for the two best poses is represented in Fig. 1, the only notable differences between the two being the positions of some hydrogen atoms.

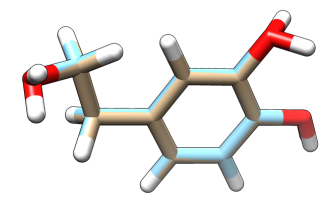
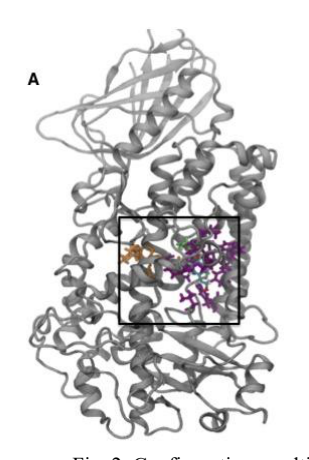


Fig. 1. Best pose for HT from the docking study of LOX5 stable form. (light blue) and from the LOX 5 apo form (beige). The overlap of the two is evident and they differ only in some of the hydrogen positions (in white).



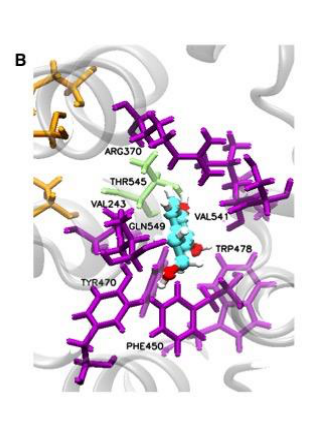


Fig. 2. Configuration resulting from the docking study: A) LOX5 represented in ribbon with the active site in yellow, the residues within a 5 Å sphere from the ligand are highlighted in purple, B) zoom of the ligand neighboring residues inside the black square in A.

The best pose of HT bound to LOX5 is shown in Fig. 2. The LOX5 residues inside a 5 Å radius from the ligand HT center of mass in the best pose, resulting from the docking experiment, are shown in Table I. We have found that they are the same for the two different docked structures LOX5 and LOX5 noFe, indicating again the same binding pose for HT in both cases. None of the residues in Table I are part of the active site of the enzyme LOX5, nor are they involved in any of the known structural characteristics of LOX5. Furthermore, the distance between the center of mass of HT and the center of mass of the catalytic site is 13.54 Å, a distance that is large enough to exclude direct interactions of the bound ligand with the active site.

TABLE I: LOX5 RESIDUES FROM THE DOCKING EXPERIMENT

Residue ResNum	
Residue ResNum	
PRO 242	
VAL 243	
THR 366	
ARG 370	
THR 371	
VAL 374	
SER 447	
LEU 448	
CYS 449	
PHE 450	
ALA 453	
ILE 454	
ARG 457	
TYR 468	
TYR 470	
TRP 478	

Therefore, the results from the docking study point to the existence of a unique binding spot for HT regardless of the composition of the catalytic site. This result is enforced by the fact that all the other poses have a consistently higher energy than the best one and are well separated in space from the best pose (cf. Tables II and III.). In particular, as reported in Table II, Model 2 and Model 3 are near to Model 1 but have a higher energy. From Model 4 on energies are clearly higher as well as RMSD values.

Finally, as it might be observe in Table III, Model 2 is very near to Model 1 but has a higher energy. From Model 3 on, energies are clearly higher as well as RMSD values.

TABLE II: AUTO DOCK VINA RESULTS FOR LOX5\_HT\_noFE

Model	Energy (Kcal/m)	RMSD		
1	-6.3	0.000		
2	-6.1	2.246		
3	-5.8	4.971		
4	-5.4	33.918		
5	-5.2	34.517		
6	-5.1	4.323		
7	-5.0	34.444		
8	-4.9	54.035		
9	-4.8	21.740		
10	-4.7	22.518		

TABLE III: AUTO DOCK VINA RESULTS FOR LOX5 HT FE

Model	Energy (Kcal/m)	RMSD
1	-6.3	0.000
2	-6.0	2.272
3	-5.5	25.879
4	-5.4	33.928
5	-5.3	53.114
6	-5.3	34.528
7	-5.2	35.494
8	-5.1	34.673
9	-5.1	53.601
10	-5.1	34.709

## B. MD Results

The apo-form of LOX5 enzyme has been studied by MD in comparison to the holo-form of the enzyme, demonstrating that the presence of iron within the active site stabilizes the conformation of human LOX5 while the apo-form of the enzyme is less stable and more able to traffick among different cell compartments (Torras et al., 2018). Additional studies document the presence of an apo-form of the enzyme LOX5 in a number of mammalian cells that contribute to traffic between different cell compartments and in the modulation of their signals (Gilbert et al., 2020).

Therefore, while the enzyme catalytic activity is surely triggered by the iron docking, conferring a stable and relatively rigid tertiary structure to the protein, many other relevant functions seem to be related to the higher degree of flexibility and adaptability shown by the iron free structure and eventually initiated by other ligand binding. We are particularly interested in the anti-inflammatory properties of LOX5 and for those reasons we have chosen to study the dynamic of the enzyme in its apo-form, in complex with HT ligand, using thus the best docking pose LOX5 noFE as starting configuration.

In the following we analyze the data resulting from molecular dynamics in the attempt to understand if HT is bound in a stable way, characterize and eventually elucidate its binding to LOX5 and its impact on LOX5 functions.

Firstly, we evaluated the dynamics of HT with respect to LOX5 by calculating the motion of the center of mass of the ligand during the simulation time. The trajectory of HT's center of mass is shown in Fig. 3.

The overall dynamics of the HT ligand shows that it does not undergo great displacements but rather oscillates around a well-defined position in a pocket made by alpha-helixes in the C-term domain of the protein which is distinct from the active site. The HT center of mass mean position is given by  $(13.53 \pm 0.55)$  Å,  $(28.5 \pm 0.42)$  Å,  $(5.36 \pm 0.34)$  Å.

We observe that the X component is slightly noisier than Y and Z ones, but overall, within a length range of less than 3 Å which is sufficiently narrow to demonstrate the absence of drift movement of the ligand's center of mass during the simulation.

The catalytic site in LOX5 is defined by the four residues HIS367, HIS372, HIS550 and ILE673 (Gilbert et al., 2011) that coordinate the iron ion. In our simulation the iron ion Fe<sup>++</sup> is not considered and accordingly the catalytic site residues should be more flexible. Visual inspection of the trajectory resulting from our MD shows that the ligand HT is always distant from the active site. To better assess this aspect we have evaluated the variation in distance between the ligand's center of mass and the catalytic site's center of mass during the simulation. The center of mass of the catalytic site is defined here as the mean position of the four aforementioned residues.

The time evolution of the distance between the ligand's center of mass and the catalytic site's center of mass is reported in Fig. 4. The mean value of this distance calculated during the MD simulation time of 217 ns is 13.62 Å with standard deviation 0.55 Å.

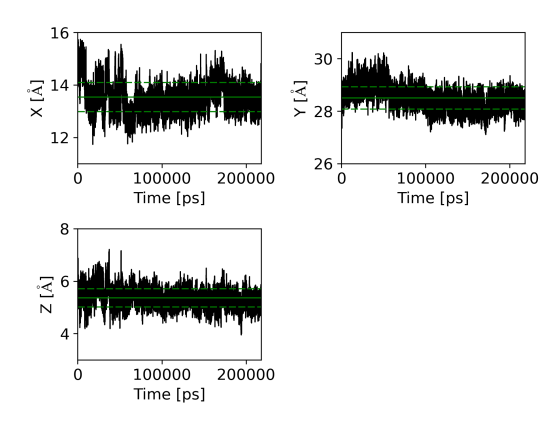


Fig. 3. Evolution of the three components of the ligand center of mass position. The vertical scale is the same for the three plots. Average values and ±1 standard deviation lines are drawn in green.

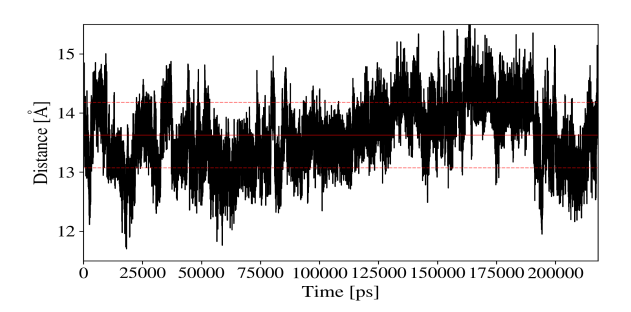


Fig. 4. Distance between HT center of mass and catalytic site center of mass. The mean value of the distance is  $13.62 \pm 0.55 \ \mbox{Å}$  and is reported as a red line in the figure with also the two  $\pm 1$  standard deviation lines.

This value suggests that there is no active interaction during the dynamics between the catalytic site and the bound ligand HT. Namely, the minimal distance is 11.6 Å, well over the typical cutoff lengths for main (Van Der Waals, dipoledipole, ionic) chemo-physical interactions forces. We thus infer that the HT molecule experiences a completely different chemical environment with respect to the active site. Moreover, due to their decay law, even long range electrostatic interactions, at such a distance, cannot make a major difference.

Next, we have evaluated the network of hydrogen bonds between HT and LOX5 during the simulation via the MD Analysis HBonds module.

In Table IV we report the only three hydrogen bonds

persistently detected during more than 50% of the MD simulation frames (liveness greater than 50%).

TABLE IV: HYDROGEN BONDS BETWEEN HT AND LOX5

Donor	Hydrogen	Acceptor	Liveness
O8 HT	H19 HT	OG1 THR545	0.98
NH1 ARG370	HH11 ARG370	O1 HT	0.71
NH1 ARG370	HH11 ARG370	H12 HT	0.63

These results show that there are only two LOX5 residues, namely ARG370 and TYR545, forming hydrogen bonds that are active along nearly the whole trajectory. TYR545 hydrogen bond involves H19 and O8 (belonging to HT) and THR545 OG1 (LOX5) and has a liveness of 98%. In ARG370 hydrogen bond we observe that the donor and hydrogen involved are the same while the acceptor switches between two different atoms of HT. This means that the hydrogen bond acceptor oscillates between two neighboring atoms of the ligand HT and thus the Hydrogen bond overall liveness is higher than the single liveness reported in the table. The presence of two stable and long-lasting hydrogen bonds means that the complex HT-LOX5 is particularly stable. To the best of our knowledge, those two residues have not been previously reported in literature as functionally important for LOX5 neither are involved in any other ligand binding to LOX5.

Finally, we have evaluated the residues of LOX5 that are found inside a radius of 5 Å from HT center of mass during the dynamics. The residues with a liveness inside this sphere higher than 90% (Table V) are almost the same as those reported from the docking study (Table I).

TABLE V: RESIDUES OF LOX5 INSIDE A RADIUS OF 5 Å FROM THE LIGAND HT DURING THE MD SIMULATION

	THE EIGAND ITI DOKING THE MID SIMOLATION			
#	Res	ResNum	Liveness	
1	GLN	549	1.0	
2	LEU	448	1.0	
3	PHE	450	1.0	
4	PHE	544	1.0	
5	THR	545	1.0	
6	VAL	243	1.0	
7	VAL	541	1.0	
8	ARG	370	0.99	
9	SER	447	0.99	
10	TYR	470	0.99	
11	TRP	478	0.98	
12	THR	366	0.95	
13	THR	371	0.94	
14	VAL	374	0.93	
15	ALA	453	0.91	
16	CYS	449	1.0	
17	ARG	457	1.0	
18	TYR	468	1.0	
19	PRO	242	1.0	
20	ILE	454	0.056	

We furtherly observe that the five LOX5 residues TYR 468, CYS 449, ARG 457, PRO242 and ILE454 found inside the 5 Å sphere in the docking study have liveness lower than 90% (reported in red in Table V). In particular, TYR468, PRO242 and ILE454 have liveness lower than 7%, thus demonstrating that they were present in the bound conformation from the docking study just because of the rigidity of the LOX5 crystal structure during the docking. During the molecular dynamic the same residues had the possibility to rearrange their positions to minimize the energy and were thus able to escape from the proximity of HT. On

the other hand, CYS449 and ARG457, which have liveness of 88%, and 75% inside the sphere, respectively, show a net propensity to stay close to the HT ligand.

Overall, these data and observations remark that HT is firmly bound to LOX5 and its environment does not change significantly during the simulation.

The hydrogen bond network analysis showed that the two most important residues for the binding of HT are TYR545 and ARG470 but, at the light of these results, we believe that also the dynamic of the residues with liveness inside the 5 Åball above 95% could be further investigated to characterize the binding pocket of HT.

## IV. CONCLUSION

In conclusion, from all the presented evidences we affirm that there is a persistent chemical bond between THR545, ARG470 and HT and that the ligand is bound in a stable manner to LOX5 in a site which is not overlapping to any other known functional site of LOX5. The presence of this new site of interaction for HT, coupled with the results from LOX5 inhibition assays, suggests an allosteric way of action of HT to modulate activity of human recombinant LOX5.

Molecules bound in allosteric sites could provoke the inhibition of LOX5. This is well explained by Gilbert et al. (2020) for the Acetyl-11-keto-beta-boswellic acid (AKBA) where it is shown that small molecules are capable of "promoting the lipid mediators class switch from proinflammatory lymphotoxins to anti-inflammatory specialized pro-resolving mediators" and this might permit new strategies for therapeutic intervention in inflammation processes.

We propose that the same line of action should be applied in our case and HT core structure and binding site information could be used for engineering bio-inspired LOX5 inhibitors, capable of inducing allosteric modulation of LOX5 activity in the cellular context and leading to diminished leukotrienes levels. We thus believe that HT, apart from the well-known dietary benefits, could be used as a scaffold to design LOX5 inhibitors with the opportunity to modulate their specificity and action.

To conclude, we are sure that the knowledge here presented about this new binding spot of HT will inspire laboratory approaches as the use of engineered LOX5 with mutated aminoacids in bioassays to demonstrate the selectivity and unicity of this binding spot, and the inhibitors design with HT structure as a scaffold to modulate their action and specificity.

## ACKNOWLEDGMENT

This work has been carried out with the financial contribution of the Sardinian Regional Authorities (BIOS project).

## CONFLICT OF INTEREST

Authors declare that they do not have any conflict of interest.

## REFERENCES

- Bertin L, Ferri F, Scoma A, et al. (2011). Recovery of high added value natural polyphenols from actual olive mill wastewater through solid phase extraction. *Chem Eng J.* 171:1287-1293.
- Bulotta S, Celano M, Lepore SM, et al. (2014). Beneficial effects of the olive oil phenolic components oleuropein and hydroxytyrosol: Focus on protection against cardiovascular and metabolic diseases. *J. Transl. Med.* 3,12:219.
- Christman LM, Gu L (2020). Efficacy and mechanisms of dietary polyphenols in mitigating rheumatoid arthritis. J. Funct. Foods. 71:104003.
- Corrêa TA, Rogero MM (2019). Polyphenols regulating microRNAs and inflammation biomarkers in obesity. *Nutrition*. 59:150-157.
- D'Angelo S, Manna C, Migliardi V, et al. (2001). Pharmacokinetics and metabolism of hydroxytyrosol, a natural antioxidant from olive oil. *Drug Metab Dispos.* 29(11):1492-1498.
- De La Puerta R, Gutierrez VR, Hoult JRS (1999). Inhibition of leukocyte 5-lipoxygenase by phenolics from virgin olive oil. *Biochem Pharmacol* 57:445–449.
- Frascari D, Bacca AEM, Zama F, et al. (2016). Olive mill wastewater valorisation through phenolic compounds adsorption in a continuous flow column. *Chem Eng J.* 283:293-303.
- Gilbert NC, Bartlett SG, Waight MT, et al. (2011). The structure of human 5-lipoxygenase. *Science*. 331(6014):217–219.
- Gilbert NC, Gerstmeier J, Schexnaydre EE, et al. (2020). Structural and mechanistic insights into 5-lipoxygenase inhibition by natural products. *Nat Chem Biol.* 16(7):783-790.
- Goldsmith CD, Bond DR, Jankowski H, et al. (2018). The olive biophenols oleuropein and hydroxytyrosol selectively reduce proliferation, influence the cell cycle, and induce apoptosis in pancreatic cancer cells. *Int J Mol Sci.* 19(7):1937.
- Han J, Talorete TPN, Yamada P, Isoda H (2009). Anti-proliferative and apoptotic effects of oleuropein and hydroxytyrosol on human breast cancer MCF-7 cells. Cytotechnology. 59(1):45-53.
- Hu T, He XW, Jiang JG, Xu XL (2014). Hydroxytyrosol and its potential therapeutic effects. *J. Agric. Food Chem.* 62(7):1449-1455.
- Humphrey W, Dalke A, Schulten K (1996). VMD: Visual molecular dynamics. *J Mol Graph*. 14:33–38.
- Jemai H, Feki AEL, Sayadi S (2009). Antidiabetic and antioxidant effects of hydroxytyrosol and oleuropein from olive leaves in alloxan-diabetic rats. J Agric Food Chem. 14;57(19):8798-8804.
- Kohyama N, Nagata T, Fujimoto SI, Sekiya K (1997). Inhibition of arachidonate lipoxygenase activities by 2-(3,4-dihydroxyphenyl)ethanol, a phenolic compound from olives. *Biosci Biotechnol Biochem* 61:347–350.
- Leri M, Natalello A, Bruzzone E, et al. (2019). Oleuropein aglycone and hydroxytyrosol interfere differently with toxic A $\beta$  1-42 aggregation. Food Chem Toxicol. 129:1-12.
- Marković AK, Torić J, Barbarić M, Brala CJ (2019). Hydroxytyrosol, tyrosol and derivatives and their potential effects on human health. *Molecules*. 24(10): 2001.
- Michaud-Agrawal N, Denning EJ, Woolf TB, Beckstein O (2011).
  MDAnalysis: A toolkit for the analysis of molecular dynamics simulations. J Comput Chem. 32(10):2319-2327.
- Newcomer ME, Brash AR (2015). The structural basis for specificity in lipoxygenase catalysis. *Protein Sci* 24:298–309.
- Nosé S (1984) A unified formulation of the constant temperature molecular dynamics methods. *J Chem Phys.* 81, 511.
- Pergola C, Werz O (2010). 5-Lipoxygenase inhibitors: A review of recent developments and patents. *Expert Opin. Ther. Pat.* 20:355–375.
- Phillips JC, Braun R, Wang W, et al. (2005). Scalable molecular dynamics with NAMD. J. Comput. Chem. 26:1781–1802.
- Romani A, Pinelli P, Ieri F, Bernini R (2016). Sustainability, innovation, and green chemistry in the production and valorization of phenolic extracts from Olea europaea L. *Sustainability*. 8, 1-10.
- Sadh PK, Duhan S, Duhan JS (2018). Agro-industrial wastes and their utilization using solid state fermentation: a review. *Bioprocess*. 5:1, 1-15.
- Schüttelkopf AW, Van Aalten DMF (2004). PRODRG: A tool for highthroughput crystallography of protein-ligand complexes. *Acta Crystallogr Sect D Biol Crystallogr*. 60(Pt 8):1355-1363.
- Serra A, Rubió L, Borràs X, et al. (2012). Distribution of olive oil phenolic compounds in rat tissues after administration of a phenolic extract from olive cake. *Mol Nutr Food Res.* 56(3):486-496.
- Sterling T, Irwin JJ (2015). ZINC 15 Ligand Discovery for Everyone. J Chem Inf Model. 55, 11, 2324–2337.

- Sun L, Luo C, Liu J (2014). Hydroxytyrosol induces apoptosis in human colon cancer cells through ROS generation. *Food Funct.* 5(8):1909-14.
- Tomé-Carneiro J, Visioli F (2016). Polyphenol-based nutraceuticals for the prevention and treatment of cardiovascular disease: Review of human evidence. *Phytomedicine*. 23(11):1145-1174.
- Trott O, Olson AJ (2009). AutoDock Vina: Improving the speed and accuracy of docking with a new scoring function, efficient optimization, and multithreading. *J Comput Chem.* 31(2): 455–461.
- Vanommeslaeghe K, Hatcher E, Acharya C, et al. (2010). CHARMM general force field: A force field for drug-like molecules compatible with the CHARMM all-atom additive biological force fields. *J Comput Chem.* 31:671–690.
- Vougogiannopoulou K, Lemus C, Halabalaki M, et al. (2014). One-step semisynthesis of oleacein and the determination as a 5-lipoxygenase inhibitor. J Nat Prod. 77:441–445.
- Zhou Y, Zheng J, Li Y, et al. (2016). Natural polyphenols for prevention and treatment of cancer. *Nutrients*. 22(8):515.
- Zubair H, Bhardwaj A, Ahmad A, et al. (2017). Hydroxytyrosol Induces Apoptosis and Cell Cycle Arrest and Suppresses Multiple Oncogenic Signaling Pathways in Prostate Cancer Cells. *Nutr Cancer*. 69(6): 932–942.
- Zurob E, Cabezas R, Villarroel E, et al. (2020). Design of natural deep eutectic solvents for the ultrasound-assisted extraction of hydroxytyrosol from olive leaves supported by COSMO-RS. Sep Purif Technol. 248:117054.